Bioorganic & Medicinal Chemistry 20 (2012) 2010–2018

Contents lists available at SciVerse ScienceDirect

Bioorganic & Medicinal Chemistry

journal homepage: www.elsevier.com/locate/bmc

Design, synthesis and biological evaluation of pyrazolyl-thiazolinone derivatives as potential EGFR and HER-2 kinase inhibitors

Ke-Ming Qiu [†], Hai-Hong Wang [†], Li-Ming Wang, Yin Luo, Xian-Hui Yang, Xiao-Ming Wang [*], Hai-Liang Zhu [*]

State Key Laboratory of Pharmaceutical Biotechnology, Nanjing University, Nanjing 210093, PR China

ARTICLE INFO

Article history:
Received 31 December 2011
Revised 26 January 2012
Accepted 27 January 2012
Available online 4 February 2012

Keywords:
Pyrazolyl-thiazolidinone
EGFR
HER-2
Antitumor
Structure–activity relationship

ABSTRACT

A series of pyrazolyl-thiazolinone derivatives (**E1–E36**) have been designed and synthesized and their biological activities were also evaluated as potential EGFR and HER-2 kinase inhibitors. Thirty-four of the 36 compounds were reported for the first time. Among them, compound 2-(5-(4-bromophenyl)-3-*p*-tolyl-4,5-dihydro-1*H*-pyrazol-1-yl)thiazol-4(5*H*)-one (**E28**) displayed the most potent inhibitory activity (IC_{50} = 0.24 μM for EGFR and IC_{50} = 1.07 μM for HER-2). Antiproliferative assay results indicated that compound **E28** owned high antiproliferative activity against MCF-7, B16-F10 and HCT-116 in vitro, with IC_{50} value of 0.30, 0.54, and 0.70 μM, respectively. Docking simulation was further performed to position compound **E28** into the EGFR active site to determine the probable binding model. Based on the preliminary results, compound **E28** with potent inhibitory activity in tumor growth would be a potential anticancer agent.

1. Introduction

Receptor protein tyrosine kinases (RPTKs), also called phosphotyrosine kinase, play a key role in signal transduction pathways that regulate cell division and differentiation. EGFR, a transmembrane protein tyrosine kinase (PTK) that is activated by ligand-induced dimerization, plays a critical role in regulating cell proliferation, differentiation, and migration.[1] EGFR family comprise four members, including: EGFR (HER-1/ErbB-1), HER-2 (ErbB-2/neu), HER-3 (ErbB-3), and HER-4 (ErbB-4).[2] EGFR tyrosine kinase-mediated cell growth signaling pathway plays an important role in the formation and development of many types of solid tumors, including head and neck, lung, breast, bladder, prostate, and kidney cancers.[3–6] Therefore, EGFR tyrosine kinase represents an attractive target for the development of novel anticancer agents. EGFR and HER-2 are the hottest targets in current cancer research and their overexpression or abnormal activation often cause cell malignant transformation.[7] Besides, they have relationship with postoperative adverse, radiotherapy and chemotherapy resistance and tumor angiogenesis.[8] Compounds that inhibit the kinase activity of EGFR and/or HER-2 after binding of its ATP binding site are of potential interest as new therapeutic antitumor agents.[9,10] Gefitinib (Iressa) and erlotinib (Tarceva) (Fig. 1) are the representative drugs for this kind of inhibitors and have been approved by US FDA for treatment of patients with non small-cell-lung cancer (NSCLC).[11,12]

Many pyrazole derivatives are acknowledged to possess a wide range of bioactivities. The pyrazole motif makes up the core structure of numerous biologically active compounds. Thus, some representatives of this heterocycle exhibit antiviral/antitumor,[13–15] antibacterial,[16,17] antiinflamatory,[18] analgesic,[19] fungistatic,[20] and anti-hyperglycemic activity.[21] Ducray et al. reported that 3-alkoxy-1*H*-pyrazolo[3,4-*d*]pyrimidines analogues (**3A-1-PP**) (Fig. 1) showed potent EGFR and HER-2 receptor tyrosine kinase inhibitory activity, with IC_{50} values reach to single digit nanomolar.[22] Besides, a series of novel pyrazole derivatives containing thiourea skeleton (**PD**, Fig. 1) were recently reported as potent anticancer agents targeting EGFR TK in our group and some of them had demonstrated potent antitumor activity.[23]

Thiazolinone and their derivatives have attracted continuing interest over the years because of their varied biological activities, such as anti-inflammatory, antimicrobial, antiproliferative, antiviral, anticonvulsant, antifungal, and antibacterial.[24–26] Recent years, thiazolinone derivatives with their antitumor activity have become a new hot spot. Havrylyuk et al. reported that thiazolidinones containing benzothiazole moiety has anticancer activity on leukemia, melanoma, lung, colon, CNS, ovarian, renal, prostate and breast cancers cell lines.[27] Moreover, our group's previous work had showed that thiazolidinone derivatives (**TD**, Fig. 1) were potent inhibitors of EGFR and HER-2.[28]

In addition, many pyrazole or thiazolinone derivatives displayed potent biological activities and low toxicities in previous reports.[23,25,28–30] But to our knowledge, few reports have been

* Corresponding authors. Tel./fax: +86 25 83592672.
E-mail address: zhuhl@nju.edu.cn (H.-L. Zhu).
† These two authors contributed equally to this paper.

0968-0896/$ - see front matter © 2012 Elsevier Ltd. All rights reserved.
doi:10.1016/j.bmc.2012.01.051

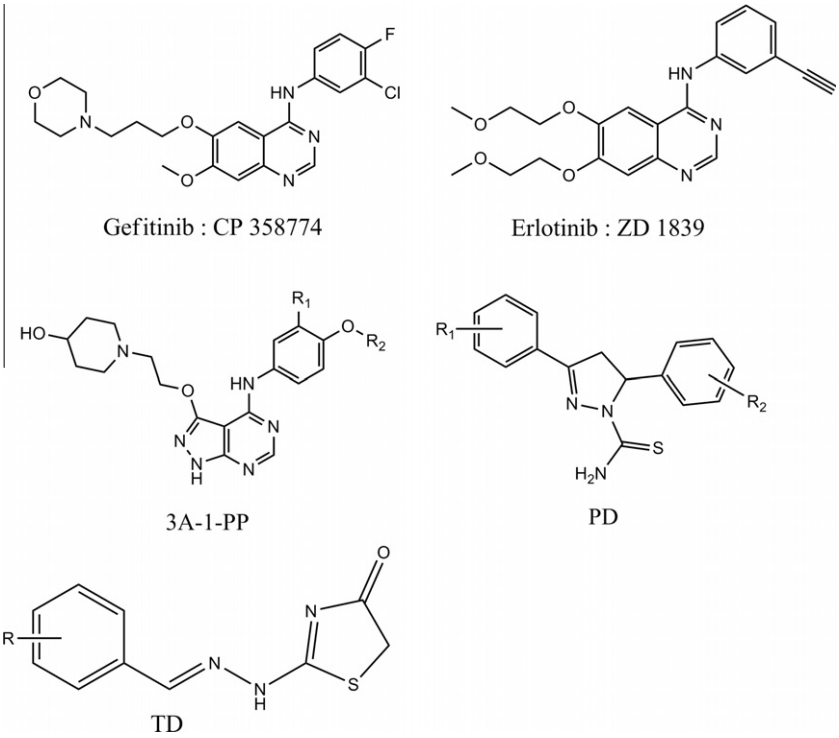

Figure 1. Chemical structures of some reported compounds.

dedicated to design and synthesize an anticancer/antitumor compound which contains pyrazole and thiazolinone simultaneously. The pyrazole ring along with the thiazolinone ring, the two combined substructures, might exhibit synergistic anticancer effect. All of these encouraged us to integrate these two heterocycles and screen new pyrazolyl-thiazolinone derivatives as potential EGFR and HER-2 inhibitory agents. Herein, we report in the present work the design, synthesis and biological evaluation of pyrazolyl-thiazolinone derivatives as potential EGFR and HER-2 kinase inhibitors. Biological evaluation indicated that some of the synthesized compounds were potent inhibitors of EGFR and HER-2.

2. Results and discussion

2.1. Chemistry

The synthesis of compounds **E1–E36** are followed the general pathway outlined in Scheme 1. Firstly, the chalcones were obtained by direct condensation by the aromatic aldehydes and the substituted acetophenone, using 40% potassium hydroxide as catalyst in ethanol. Secondly, cyclization of different chalcones with thiosemicarbazide under basic condition leads to the formation of pyrazole derivatives containing thiourea skeleton. Thirdly, pyrazolyl-thiazolinone derivatives **E1–E42** were obtained by reacting compound **D** (1 equiv) with bromoacetic acid (1.2 equiv) in acetic acid and keeping under stirring at 80 °C for 6–8 h. Moreover, acetic anhydride (2 equiv) was added as dehydrating agent and sodium acetate (2 equiv) was used as acid-binding agent. Among these compounds, **E1–E5**, **E7–E20** and **E22–E36** are reported for the first time. All of the synthetic compounds gave satisfactory analytical and spectroscopic data, which were in full accordance with their depicted structures.

2.2. In vitro enzyme inhibition activity

The synthesized derivatives were evaluated for their ability to inhibit the autophosphorylation of EGFR and HER-2 kinases using

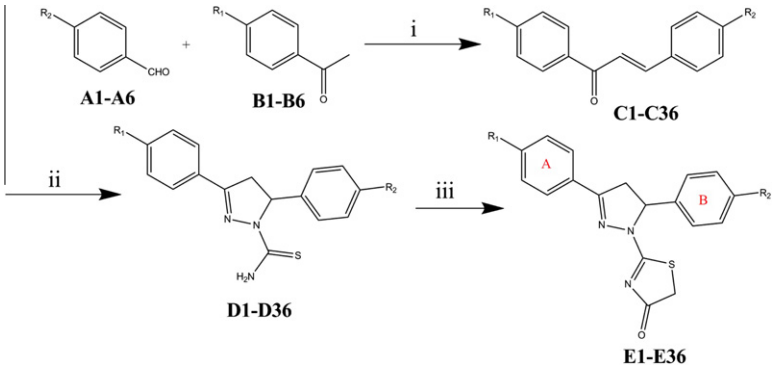

Scheme 1. General synthesis of pyrazolyl-thiazolinone derivatives (**E1–E36**). Reagents and conditions: (i) 40% aqueous potassium hydroxide solution, ethanol, rt; (ii) thiosemicarbazide, KOH, ethanol, reflux; (iii) bromoacetic acid, acetic anhydride, sodium acetate, acetic acid, 80 °C, 6–8 h.

a solid-phase ELISA assay. The results were summarized in Table 2. It was observed that pyrazolyl-thiazolinone derivatives containing thiazolinone and pyrazoline rings showed fairly good inhibiting EGFR activities displaying IC_{50} values between 0.24 and 16.92 μM. Among them, compound **E28** displayed the most potent inhibitory activity (IC_{50} = 0.24 μM for EGFR and IC_{50} = 1.07 μM for HER-2). Subsequently SAR studies were performed by modification of the parent compound to determine how the substituents of the subunits affect the EGFR inhibitory activities. Inspection of the chemical structures of the compounds **E1–E36** suggested that they could be divided into two subunits: A- and B-rings (Scheme 1 and Table 1).

As showed in Table 2, structure–activity relationships in compounds **E1–E36** demonstrated that compounds bearing one methyl group at *para*-position at A-ring showed better EGFR and HER-2 inhibitory activity (**E25–E30**, IC_{50} = 0.24–4.24 μM for EGFR and IC_{50} = 1.07–6.23 μM for HER-2) than those with hydrogen (**E1–E6**), fluorin (**E7–E12**), chlorine (**E13–E18**), bromine (**E19–E24**) and methoxyl (**E31–E36**) substituents, basically in the order of Me > H > Br > Cl > F and Me > OMe. This meant that compound with a faintish electron-donating substituents at *para*-position of A-ring (*para*-Me) had better EGFR activity than that with a relatively stronger electron-donating substituents (*para*-OMe). We could also get the result that a methyl group at the *para*-position (compound **E25–E30**) of A ring might have slightly improved EGFR inhibitory activity compared to a hydrogen atom at the same position (compound **E1–E6**), whereas a halogen atom at the same position led to a noteworthy loss of activity, which was an electron-withdrawing substituent.

In the case of constant A ring substituents, changes of substituents on B ring can also affect the activities of these compounds. Contrary to A ring, bromine at *para*-position derivatives had the best activity (IC_{50} = 0.24–4.79 μM for EGFR, and IC_{50} = 1.07–6.24 μM for HER-2), which was a faintish electron-withdrawing substituent. While a significant loss of activity was observed when the bromine atom was replaced by a chlorine/fluorine atom (IC_{50} = 1.66–10.92 μM/2.01–16.92 μM; 3.11–13.16 μM/3.53–18.12 μM for EGFR and HER-2, respectively), which was a relatively strong electron-withdrawing substituent. Moreover, with a Me/OMe group at *para*-position showed relatively poor activity (IC_{50} = 1.16–8.36 μM/4.24–10.69 μM for EGFR, IC_{50} = 2.52–10.26 μM/6.23–12.43 μM for HER-2, respectively), and this due to its electron-donating effect.

Herein, at the same position for the given compounds, we observed that the IC_{50} value for inhibition of HER-2 kinase was, in general, higher than that observed for EGFR kinase but had the same trends. This was possibly due, in part, to the fact that in the enzyme assays we used higher concentration of the purified HER-2 kinase than EGFR kinase. It was evident that there was also a reasonable correlation between the EGFR and HER-2 inhibitory activities. Thus, this was not surprising in view of the high sequence homology of the catalytic domains of these two kinases. Among all the compounds **E1–E36**, compound **E28** (IC_{50} = 0.24 μM for EGFR and IC_{50} = 1.07 μM for HER-2) showed the best activity while the substituents in the A ring and B ring are respectively methyl and bromine substituents at *para*-position.

The above results indicated that thiazolinone and pyrazoline rings in the pyrazolyl-thiazolinone derivatives might play an important role in the EGFR and HER-2 inhibitory activity. However, the changes of substituents on the benzene rings had effects on the activity of the compound, but it was not so obviously as possible. This might be explained that substituents on the benzene rings had limited influence on the molecular bonding between the protein and the compounds. Molecular docking of all the compounds of this series had demonstrated this point and this was conformed to our estimate. Nevertheless, the thiazolinone and pyrazoline different from classical EGFR inhibitors (e.g., gefitinib and erlotinib) with their potential EGFR inhibit effect could be the parent nucleus of novel efficient EGFR inhibitors.

Table 1
Chemical structures of pyrazolyl-thiazolinone derivatives

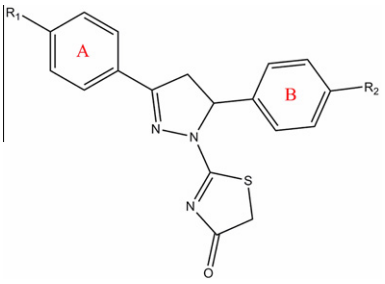

Compounds	R_1	R_2	Compounds	R_1	R_2
E1	H	H	**E19**	Br	H
E2	H	F	**E20**	Br	F
E3	H	Cl	**E21**	Br	Cl
E4	H	Br	**E22**	Br	Br
E5	H	Me	**E23**	Br	Me
E6	H	OMe	**E24**	Br	OMe
E7	F	H	**E25**	Me	H
E8	F	F	**E26**	Me	F
E9	F	Cl	**E27**	Me	Cl
E10	F	Br	**E28**	Me	Br
E11	F	Me	**E29**	Me	Me
E12	F	OMe	**E30**	Me	OMe
E13	Cl	H	**E31**	OMe	H
E14	Cl	F	**E32**	OMe	F
E15	Cl	Cl	**E33**	OMe	Cl
E16	Cl	Br	**E34**	OMe	Br
E17	Cl	Me	**E35**	OMe	Me
E18	Cl	OMe	**E36**	OMe	OMe

2.3. Antiproliferative activity and molecular docking study

The in vitro antiproliferative activities of nine compounds (**E4, E16, E22, E25–E29**, **E34**) with better inhibition activities against EGFR were tested using MCF-7, B16-F10, and HCT-116 cancer cell lines. As was shown in Table 3, out of the top nine compounds, compounds **E28** and **E25**, which had potent inhibitory activity of EGFR showed high antiproliferative activity (IC_{50} = 0.30 and 0.73 μM for MCF-7, IC_{50} = 0.54 and 0.86 μM for B16-F10, IC_{50} = 0.70 and 1.16 μM for HCT-116), indicating that these pyrazolyl-thiazolinone derivatives were potent antitumor agents. In particular, compound **E28** had demonstrated significant inhibitory activity in tumor growth inhibition and displayed potential EGFR inhibitory activity.

To gain better understanding on the potency of the compound **E28** and guide further SAR studies, we proceeded to examine the interaction of it with EGFR (PDB code: 1M17) by molecular docking, which was performed by simulation of the compound into the ATP binding site in EGFR. The binding model of compound **E28** and EGFR was depicted in Figure 2A. The amino acid residues which had interaction with EGFR were labeled. In the binding mode, compound **E28** was nicely bound to the ATP binding site of EGFR through hydrophobic interaction and the binding was stabilized by a hydrogen bond and a π–cation interaction.

In the binding model, compound **E28** was nicely bound to the EGFR kinase with its carbonyl group project toward the trunk chain amino-group of A721 (LYS 721), forming a more optimal H-bond interaction (distance: N–H···O = 1.93 Å, angle: 118.7°). Based on the favorable EGFR inhibitory activity of pyrazolyl-thiazolinone derivatives, it could be concluded that this H-bond played an important effect in the EGFR inhibitory. The end amino cation of

Table 2
Inhibition activities of compounds **E1**–**E42** against EGFR and HER-2 (IC_{50}, μM)

Compounds	EGFR	HER-2	Compounds	EGFR	HER-2
E1	3.38 ± 0.34	5.12 ± 0.58	**E19**	3.20 ± 0.35	4.87 ± 0.52
E2	4.86 ± 0.50	6.35 ± 0.65	**E20**	6.48 ± 0.70	8.14 ± 0.83
E3	3.49 ± 0.32	4.83 ± 0.45	**E21**	4.12 ± 0.45	5.87 ± 0.60
E4	1.35 ± 0.12	3.05 ± 0.33	**E22**	2.03 ± 0.21	3.65 ± 0.35
E5	3.03 ± 0.35	4.64 ± 0.42	**E23**	5.58 ± 0.52	7.04 ± 0.72
E6	4.27 ± 0.45	6.21 ± 0.70	**E24**	7.96 ± 0.82	9.27 ± 1.01
E7	8.14 ± 0.86	10.53 ± 0.98	**E25**	1.08 ± 0.13	2.24 ± 0.25
E8	16.92 ± 1.58	18.12 ± 1.69	**E26**	2.01 ± 0.22	3.53 ± 0.33
E9	10.92 ± 1.11	13.16 ± 1.46	**E27**	1.66 ± 0.18	3.11 ± 0.33
E10	4.79 ± 0.51	6.24 ± 0.58	**E28**	0.24 ± 0.04	1.07 ± 0.12
E11	8.36 ± 0.85	10.26 ± 1.12	**E29**	1.16 ± 0.12	2.52 ± 0.23
E12	10.69 ± 1.12	12.43 ± 1.36	**E30**	4.24 ± 0.45	6.23 ± 0.68
E13	5.34 ± 0.55	7.05 ± 0.73	**E31**	2.37 ± 0.23	4.12 ± 0.43
E14	14.21 ± 1.41	16.42 ± 1.73	**E32**	5.95 ± 0.64	8.04 ± 0.86
E15	8.16 ± 0.86	9.96 ± 1.02	**E33**	5.35 ± 0.55	7.59 ± 0.77
E16	2.28 ± 0.24	3.84 ± 0.42	**E34**	1.26 ± 0.15	2.75 ± 0.24
E17	6.67 ± 0.72	8.13 ± 0.85	**E35**	5.46 ± 0.58	7.35 ± 0.75
E18	8.58 ± 0.84	10.34 ± 1.12	**E36**	8.89 ± 0.91	10.48 ± 1.13
Erlotinib	0.03 ± 0.002	0.14 ± 0.02			

Table 3
Antiproliferative activities of compounds **E4**, **E16**, **E22**, **E25**–**E29**, **E34** (IC_{50}, μM)

Compounds	MCF-7	B16-F10	HCT-116
E3	0.93 ± 0.08	1.40 ± 0.13	1.70 ± 0.13
E16	2.12 ± 0.19	2.10 ± 0.18	2.34 ± 0.18
E22	2.13 ± 0.23	1.49 ± 0.15	2.19 ± 0.24
E25	0.73 ± 0.08	0.86 ± 0.06	1.16 ± 0.10
E26	1.83 ± 0.19	1.50 ± 0.12	1.93 ± 0.21
E27	1.53 ± 0.15	1.22 ± 0.12	1.79 ± 0.18
E28	0.30 ± 0.41	0.54 ± 0.04	0.70 ± 0.08
E29	1.17 ± 0.13	1.01 ± 0.08	1.26 ± 0.13
E34	1.51 ± 0.17	2.68 ± 0.22	3.92 ± 0.41
Erlotinib	0.07 ± 0.008	0.10 ± 0.012	0.14 ± 0.012

LYS721 was also formed a π–cation interaction with the benzene ring of compound **E28** (distance: 4.53 Å), which enhanced the binding action between receptor EGFR and ligand compound **E28**. The electron-donating substituent amino-NH_2 strengthened the π–cation binding and the results indicated that it was primarily due to direct through-space interaction between the substituent and the cation.

Meanwhile, we chose erlotinib as the positive control in the docking procedure. In Figure 2B, it was found that there was only one sigma–π bond in the binding pocket. The benzene ring of erlotinib formed one sigma–π bond with VAL702 (distance: 2.80 Å). The model between compound **E28** and the ATP binding site was similar to that with erlotinib. Comparing these models, it was found that the hydrophobic pockets of ATP binding site were all nicely occupied by these compounds, and the difference was the combination mode. This molecular docking result, along with the biological assay data, suggesting that compound **E28** was a potential inhibitor of EGFR.

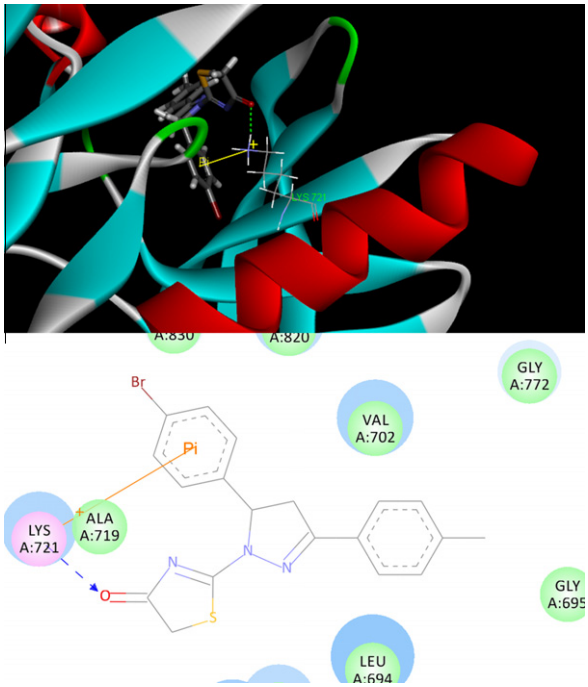

Figure 2A. Molecular docking modeling of compound **E28** with EGFR kinase: for clarity, only interacting residues are displayed. Above: 3D model of the interaction between compound **E28** and the ATP binding site. The H-bond (green lines) is displayed as dotted lines, and the π–cation interaction is shown as yellow lines. Below: 2D model of the interaction between compound **E28** and the ATP binding site. The H-bond (blue arrows) is displayed as dotted arrows, and the π–cation interaction is shown as orange lines.

3. Conclusions

In this paper, a series of pyrazolyl-thiazolinone derivatives that may function as inhibitors of EGFR and HER-2 kinases have been synthesized and their biological activities were evaluated. And some of them displayed potent EGFR and HER-2 inhibitory activities and antiproliferative activities against MCF-7 cell lines, B16-F10 cell lines and HCT-116 cell lines. Among them, compound **E28** showed the most potent EGFR inhibition activities (IC_{50} = 0.24 μM for EGFR and IC_{50} = 1.07 μM for HER-2) and anticancer activities (IC_{50} = 0.30 μM for MCF-7, IC_{50} = 0.54 μM for B16-F10 and IC_{50} = 0.70 μM for HCT-116).

Molecular docking was further performed to study the inhibitor-EGFR protein interactions. After analysis of the binding model of compound **E28** with EGFR, it was found that a hydrogen bond and a π–cation interaction with the protein residues in the ATP binding site might play a crucial role in its EGFR inhibition and antiproliferative activities. Among these compounds, it could be concluded that compound **E28** had been demonstrated to show significant EGFR and tumor growth inhibitory activity as a potential anticancer agent. The result of this work might be helpful for

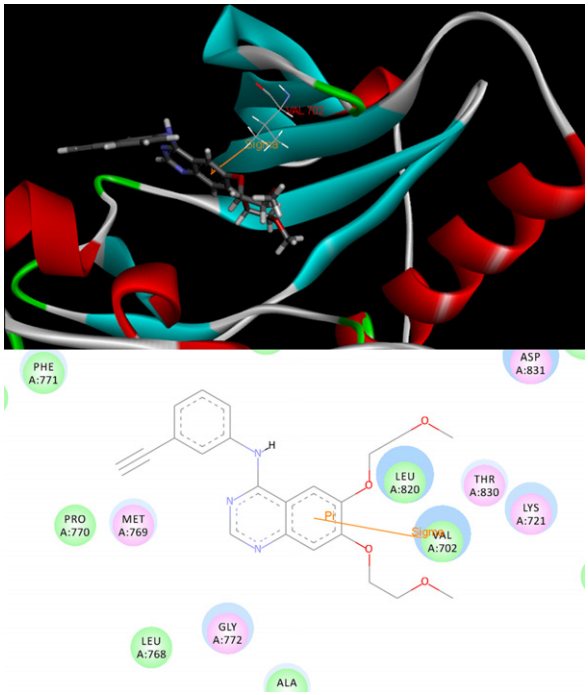

Figure 2B. Molecular docking modeling of erlotinib with EGFR kinase: or clarity, only interacting residues are displayed. Above: 3D model of the interaction between erlotinib and the ATP binding site. The π–sigma bond is displayed as orange lines. Below: 2D model of the interaction between erlotinib and the ATP binding site. The π–sigma bond is displayed as orange lines.

the design and synthesis of EGFR inhibitors with stronger activities.

4. Experiments

4.1. Materials and measurements

All chemicals and reagents used in current study were of analytical grade. All the ^{1}H NMR spectra were recorded on a Bruker DPX300 model Spectrometer in $CDCl_3$ or DMSO-d_6 and chemical shifts were reported in ppm (δ). ESI-MS spectra were performed on a CHN-O-Rapid instrument. TLC was performed on the glass-backed silica gel sheets (Silica Gel 60 GF254) and visualized in UV light (254 nm). Column chromatography was performed using silica gel (200–300 mesh) eluting with ethyl acetate and petroleum ether.

4.2. Synthesis

4.2.1. General synthetic procedure of chalcones (C1–C36)

Equimolar portions of the appropriately aromatic aldehydes (3 mmol, 1 equiv) and substituted acetophenone (3 mmol, 1 equiv) were dissolved in approximately 20 mL of ethanol. The mixture was allowed to stir for several minutes at 0 °C to let dissolve. Than a 1 mL aliquot of a 40% aqueous potassium hydroxide solution was then slowly added dropwise to the reaction flask via a self-equalizing addition funnel. The reaction solution was allowed to stir at room temperature for approximately 4–6 h. Most commonly, a precipitate formed and was then collected by suction filtration.

4.2.2. General synthetic procedure of pyrazole derivatives (D1–D36)

A mixture of chalcone (2 mmol), thiosemicarbazide (3 mmol), and KOH (2 mmol) was refluxed in ethanol (30 mL) for 12 h. After cooling, the solution was poured into mass of ice-water and stirred for a few minutes. The precipitate was filtered and crystallized from ethanol.

4.2.3. General synthetic procedure of pyrazolyl-thiazolinone derivatives (E1–E36)

A mixture of compound **D** (1 mmol), bromoacetic acid (1.2 mmol), acetic anhydride (2 mmol), and sodium acetate (2 mmol) was dissolved in acetic acid (20 mL) and kept stirring in 80 °C for 6–8 h. After cooling, the solution was poured into mass of ice-water and stirred for a few minutes. The precipitate was filtered and crystallized from methylene dichloride/ethanol = 1:1.

4.2.3.1. 2-(3,5-Diphenyl-4,5-dihydro-1*H*-pyrazol-1-yl)thiazol-4(5*H*)-one (E1). Yield 65%; mp 208–210 °C. ^{1}H NMR ($CDCl_3$, 300 MHz): 3.38 (dd, J_1 = 4.02 Hz, J_2 = 18.04 Hz, 1H), 3.87 (s, 2H), 3.97 (dd, J_1 = 7.04 Hz, J_2 = 15.56 Hz, 1H), 5.86 (s, 1H), 7.25–7.30 (m, 3H), 7.45–7.52 (m, 3H), 7.46 (d, J = 8.02 Hz, 2H),7.62(d, J = 5.34 Hz, 2H). ESI-MS: 322.40 ($C_{18}H_{16}N_3OS$, $[M+H]^+$). Anal. Calcd for $C_{18}H_{15}N_3OS$: C, 67.27; H, 4.70; N, 13.07. Found: C, 67.38; H, 4.72; N, 13.13.

4.2.3.2. 2-(5-(4-Fluorophenyl)-3-phenyl-4,5-dihydro-1*H*-pyrazol-1-yl)thiazol-4(5*H*)-one (E2). Yield 70%; mp 213–215 °C. ^{1}H NMR ($CDCl_3$, 300 MHz): 3.38 (d, J = 16.83 Hz, 1H), 3.85 (s, 2H), 3.95 (dd, J_1 = 7.14 Hz, J_2 = 14.28 Hz, 1H), 5.83 (d, J = 8.79 Hz, 1H), 7.14–7.17 (m, 4H), 7.44–7.51 (m, 3H), 7.80 (d, J = 6.6 Hz, 2H). ESI-MS: 340.39 ($C_{18}H_{15}FN_3OS$, $[M+H]^+$). Anal. Calcd for $C_{18}H_{14}FN_3OS$: C, 63.70; H, 4.16; N, 12.38. Found: C, 63.57; H, 4.14; N, 12.33.

4.2.3.3. 2-(5-(4-Chlorophenyl)-3-phenyl-4,5-dihydro-1*H*-pyrazol-1-yl)thiazol-4(5*H*)-one (E3). Yield 70%; mp 218–220 °C. ^{1}H NMR ($CDCl_3$, 300 MHz): 3.71 (dd, J_1 = 6.96 Hz, J_2 = 14.10 Hz, 1H), 3.86 (s, 2H), 4.11 (dd, J_1 = 7.14 Hz, J_2 = 14.28 Hz, 1H), 5.79 (s, 1H), 7.19 (d, J = 8.04, 2H), 7.30 (d, J = 7.68, 2H), 7.45–7.52 (m, 3H), 7.79 (d, J = 7.68 Hz, 2H). ESI-MS: 356.84 ($C_{18}H_{15}ClN_3OS$, $[M+H]^+$). Anal. Calcd for $C_{18}H_{14}ClN_3OS$: C, 60.76; H, 3.97; N, 11.81. Found: C, 60.64; H, 3.96; N, 11.76.

4.2.3.4. 2-(5-(4-Bromophenyl)-3-phenyl-4,5-dihydro-1*H*-pyrazol-1-yl)thiazol-4(5*H*)-one (E4). Yield 72%; mp 244–246 °C. ^{1}H NMR ($CDCl_3$, 300 MHz): 3.37 (d, J = 16.83 Hz, 1H), 3.87 (s, 2H), 4.11(dd, J_1 = 7.14 Hz, J_2 = 14.25 Hz, 1H), 5.81 (s, 1H), 7.15 (d, J = 7.86 Hz, 2H), 7.45–7.52 (m, 5H), 7.80 (d, J = 7.32 Hz, 2H). ESI-MS: 401.29 ($C_{18}H_{15}BrN_3OS$, $[M+H]^+$). Anal. Calcd for $C_{18}H_{14}BrN_3OS$: C, 54.01; H, 3.53; N, 10.50. Found: C, 54.16; H, 3.55; N, 10.56.

4.2.3.5. 2-(3-Phenyl-5-(*p*-tolyl)-4,5-dihydro-1*H*-pyrazol-1-yl)thiazol-4(5*H*)-one (E5). Yield 75%; mp 213–215 °C. ^{1}H NMR ($CDCl_3$, 300 MHz): 2.04 (s, 3H), 3.37 (dd, J_1 = 3.66 Hz, J_2 = 17.91 Hz, 1H), 3.87 (s, 2H), 3.97 (dd, J_1 = 6.39 Hz, J_2 = 17.55 Hz, 1H), 5.88 (d, J = 10.08 Hz, 1H), 7.02 (t, J = 8.58 Hz, 2H), 7.24–7.28 (m, 1H), 7.45–7.52 (m, 3H), 7.79–7.83 (m, 2H). ESI-MS: 336.42 ($C_{19}H_{18}N_3OS$, $[M+H]^+$). Anal. Calcd for $C_{19}H_{17}N_3OS$: C, 68.03; H, 5.11; N, 12.53. Found: C, 68.18; H, 5.13; N, 12.61.

4.2.3.6. 2-(5-(4-Methoxyphenyl)-3-phenyl-4,5-dihydro-1*H*-pyrazol-1-yl)thiazol-4(5*H*)-one (E6). Yield 76%; mp 214–216 °C. ^{1}H NMR ($CDCl_3$, 300 MHz): 3.41(d, J = 10.62 Hz, 1H), 3.87 (s, 3H), 3.92 (s, 2H), 3.96 (dd, J_1 = 4.24 Hz, J_2 = 14.23 Hz, 1H), 5.99 (s, 1H), 6.85 (d, J = 5.04 Hz, 2H), 7.25 (d, J = 3.93 Hz, 2H), 7.47–7.50 (m, 2H), 7.52 (d, J = 4.41 Hz, 1H), 7.82 (d, J = 4.47 Hz, 2H). ESI-MS: 352.42 ($C_{19}H_{18}N_3O2S$, $[M+H]^+$). Anal. Calcd for $C_{19}H_{17}N_3O_2S$: C, 64.94; H, 4.88; N, 11.96. Found: C, 64.99; H, 4.87; N, 12.01.

4.2.3.7. 2-(3-(4-Fluorophenyl)-5-phenyl-4,5-dihydro-1*H*-pyrazol-1-yl)thiazol-4(5*H*)-one (E7). Yield 68%; mp 232–235 °C. ^{1}H NMR ($CDCl_3$, 300 MHz): 3.37 (dd, J_1 = 8.28 Hz, J_2 = 14.24 Hz, 1H), 3.87 (s, 2H), 3.95 (dd, J_1 = 5.94 Hz, J_2 = 17.24 Hz, 1H), 5.84 (d, J = 10.04 Hz, 1H), 7.24 (s, 1H), 7.31 (d, J = 4.28 Hz, 2H), 7.28–7.36 (m, 4H), 7.83 (d, J = 8.24 Hz, 2H). ESI-MS: 340.39 ($C_{18}H_{15}FN_3OS$, $[M+H]^+$). Anal. Calcd for $C_{18}H_{14}FN_3OS$: C, 63.70; H, 4.16; N, 12.38. Found: C, 63.85; H, 4.18; N, 12.45.

4.2.3.8. 2-(3,5-Bis(4-fluorophenyl)-4,5-dihydro-1*H*-pyrazol-1-yl)thiazol-4(5*H*)-one (E8). Yield 80%; mp 247–249 °C. ^{1}H NMR ($CDCl_3$, 300 MHz): 3.35 (d, J = 15.35 Hz, 1H), 3.87 (s, 2H), 3.96 (d, J = 17.19 Hz, 1H), 5.82 (d, J = 9.33 Hz, 1H), 6.91–7.05 (m, 2H), 7.14–7.17 (m, 2H), 7.20–7.24 (m, 2H), 7.60–7.83 (m, 2H). ESI-MS: 358.38 ($C_{18}H_{14}F_2N_3OS$, $[M+H]^+$). Anal. Calcd for $C_{18}H_{13}F_2N_3OS$: C, 60.49; H, 3.67; N, 11.76. Found: C, 60.37; H, 3.66; N, 11.70.

4.2.3.9. 2-(5-(4-Chlorophenyl)-3-(4-fluorophenyl)-4,5-dihydro-1*H* -pyrazol-1-yl)thiazol-4(5*H*)-one (E9). Yield 82%; mp 256–258 °C. ^{1}H NMR ($CDCl_3$, 300 MHz): 3.33 (d, J = 14.07 Hz, 1H), 3.87 (s, 2H), 3.96 (d, J = 17.37 Hz, 1H), 5.79 (d, J = 7.5 Hz, 1H), 6.91–7.13 (m, 4H), 7.31 (d, J = 8.25 Hz, 2H), 7.60–7.82 (m, 2H). ESI-MS: 374.83 ($C_{18}H_{14}ClFN_3OS$, $[M+H]^+$). Anal. Calcd for $C_{18}H_{13}ClFN_3OS$: C, 57.83; H, 3.51; N, 11.24. Found: C, 57.74; H, 3.52; N, 11.19.

4.2.3.10. 2-(5-(4-Bromophenyl)-3-(4-fluorophenyl)-4,5-dihydro-1*H* -pyrazol-1-yl)thiazol-4(5*H*)-one (E10). Yield 83%; mp 262–264 °C. ^{1}H NMR ($CDCl_3$, 300 MHz): 3.33 (d, J = 17.16 Hz, 1H), 3.87–3.99 (m, 3H), 5.84 (s, 1H), 7.02 (d, J = 8.61 Hz, 1H), 7.13–7.20 (m, 2H), 7.22–7.26 (m, 1H), 7.47 (d, J = 8.22 Hz, 1H), 7.60–7.68 (m, 2H), 7. 80 (dd, J_1 = 5.31 Hz, J_2 = 8.79 Hz, 1H). ESI-MS: 419.28 ($C_{18}H_{14}BrFN_3OS$, $[M+H]^+$). Anal. Calcd for $C_{18}H_{13}BrFN_3OS$: C, 51.69; H, 3.13; N, 10.05. Found: C, 51.58; H, 3.13; N, 10.01.

4.2.3.11. 2-(3-(4-Fluorophenyl)-5-(*p*-tolyl)-4,5-dihydro-1*H* -pyrazol-1-yl)thiazol-4(5*H*)-one (E11). Yield 80%; mp 229–231 °C. ^{1}H NMR ($CDCl_3$, 300 MHz): 2.31 (s, 3H), 3.35 (d, J = 14.64 Hz, 1H), 3.85 (s, 2H), 3.94 (d, J = 17.01 Hz, 1H), 5.83 (d, J = 8.22 Hz, 1H), 7.14–7.19 (m, 6H), 7. 81 (dd, J_1 = 5.28 Hz, J_2 = 8.76 Hz, 2H). ESI-MS: 354.41 ($C_{19}H_{17}FN_3OS$, $[M+H]^+$). Anal. Calcd for $C_{19}H_{16}FN_3OS$: C, 64.57; H, 4.56; N, 11.89. Found: C, 64.65; H, 4.59; N, 11.94.

4.2.3.12. 2-(3-(4-Fluorophenyl)-5-(4-methoxyphenyl)-4,5-dihydro-1*H* -pyrazol-1-yl)thiazol-4(5*H*)-one (E12). Yield 85%; mp 240–242 °C. ^{1}H NMR ($CDCl_3$, 300 MHz): 3.37 (d, J = 17.01 Hz, 1H), 3.67 (s, 2H), 3.76 (s, 3H), 4.10 (dd, J_1 = 6.93 Hz, J_2 = 15.62 Hz, 1H), 5.83 (d, J = 10.24, 1H), 6.85 (d, J = 8.40 Hz, 2H), 7.14–7.22 (m, 4H), 7.81 (dd, J_1 = 5.31 Hz, J_2 = 8.61 Hz, 2H). ESI-MS: 370.41 ($C_{19}H_{17}FN_3O_2S$, $[M+H]^+$). Anal. Calcd for $C_{19}H_{16}FN_3O_2S$: C, 61.77; H, 4.37; N, 11.37. Found: C, 61.62; H, 4.36; N, 11.32.

4.2.3.13. 2-(3-(4-Chlorophenyl)-5-phenyl-4,5-dihydro-1*H* -pyrazol-1-yl)thiazol-4(5*H*)-one (E13). Yield 70%; mp 236–238 °C. ^{1}H NMR ($CDCl_3$, 300 MHz): 3.35 (dd, J_1 = 3.66 Hz, J_2 = 17.73 Hz, 1H), 3.92 (s, 2H), 4.12 (dd, J_1 = 7.14 Hz, J_2 = 14.28 Hz, 1H), 5.82(d, J = 7.50 Hz, 1H), 7.22–7.26 (m, 2H), 7.31–7.39 (m, 3H), 7.44 (d, J = 8.58 Hz, 2H), 7.73 (d, J = 11.70 Hz, 2H). ESI-MS: 356.84 ($C_{18}H_{15}ClN_3OS$, $[M+H]^+$). Anal. Calcd for $C_{18}H_{14}ClN_3OS$: C, 60.76; H, 3.97; N, 11.81. Found: C, 60.58; H, 3.95; N, 11.70.

4.2.3.14. 2-(3-(4-Chlorophenyl)-5-(4-fluorophenyl)-4,5-dihydro-1*H* -pyrazol-1-yl)thiazol-4(5*H*)-one (E14). Yield 81%; mp 245–247 °C. ^{1}H NMR ($CDCl_3$, 300 MHz): 3.37 (s, 1H), 3.73–3.87 (m, 3H), 5.79 (d, J = 8.24 Hz, 1H), 7.03 (d, J = 7.32 Hz, 2H), 7.26 (s, 2H), 7.44 (d, J = 7.86 Hz, 2H), 7.74 (d, J = 8.40 Hz, 2H). ESI-MS: 374.83 ($C_{18}H_{14}ClFN_3S$, $[M+H]^+$). Anal. Calcd for $C_{18}H_{13}ClFN_3S$: C, 57.83; H, 3.51; N, 11.24. Found: C, 57.71; H, 3.49; N, 11.27.

4.2.3.15. 2-(3,5-Bis(4-chlorophenyl)-4,5-dihydro-1*H*-pyrazol-1-yl)thiazol-4(5*H*)-one (E15). Yield 82%; mp 253–255 °C. ^{1}H NMR ($CDCl_3$, 300 MHz): 3.32 (d, J = 17.37 Hz, 1H), 3.87 (s, 2H), 4.12 (dd, J_1 = 7.14 Hz, J_2 = 14.28 Hz, 1H), 5.79 (s, 1H), 7.19 (d, J = 8.22 Hz, 2H), 7.31 (d, J = 8.07 Hz, 2H), 7.45 (d, J = 8.22 Hz, 2H), 7.73 (d, J = 8.61 Hz, 2H). ESI-MS: 391.29 ($C_{18}H_{14}Cl_2N_3OS$, $[M+H]^+$). Anal. Calcd for $C_{18}H_{13}Cl_2N_3OS$: C, 55.39; H, 3.36; N, 10.77. Found: C, 55.23; H, 3.34; N, 10.71.

4.2.3.16. 2-(5-(4-Bromophenyl)-3-(4-chlorophenyl)-4,5-dihydro-1*H* -pyrazol-1-yl)thiazol-4(5*H*)-one (E16). Yield 80%; mp 257–259 °C. ^{1}H NMR ($CDCl_3$, 300 MHz): 3.32 (d, J = 17.37 Hz, 1H), 3.87 (s, 2H), 4.12 (dd, J_1 = 7.14 Hz, J_2 = 14.28 Hz, 1H), 5.78 (s, 1H), 7.13 (d, J = 8.22 Hz, 2H), 7.44–7.48 (m, 4H), 7.43 (d, J = 8.43 Hz, 2H). ESI-MS: 435.74 ($C_{18}H_{14}BrClN_3OS$, $[M+H]^+$). Anal. Calcd for $C_{18}H_{13}BrClN_3OS$: C, 49.73; H, 3.01; N, 9.67. Found: C, 49.61; H, 3.02; N, 9.74.

4.2.3.17. 2-(3-(4-Chlorophenyl)-5-(p-tolyl)-4,5-dihydro-1*H* -pyrazol-1-yl)thiazol-4(5*H*)-one (E17). Yield 85%; mp 242–244 °C. ^{1}H NMR ($CDCl_3$, 300 MHz): 2.31(s, 3H), 3.38 (d, J = 12.74 Hz, 1H), 3.86–3.95 (m, 3H), 5.81 (s, 1H), 7.13–7.15 (m, 4H), 7.44 (d, J = 8.04 Hz, 2H), 7.73 (d, J = 8.43 Hz, 2H). ESI-MS: 370.87 ($C_{19}H_{17}ClN_3OS$, $[M+H]^+$). Anal. Calcd for $C_{19}H_{16}ClN_3OS$: C, 61.70; H, 4.36; N, 11.36. Found: C, 61.92; H, 4.39; N, 11.44.

4.2.3.18. 2-(3-(4-Chlorophenyl)-5-(4-methoxyphenyl)-4,5-dihydro-1*H* -pyrazol-1-yl)thiazol-4(5*H*)-one (E18). Yield 85%; mp 245–247 °C. ^{1}H NMR ($CDCl_3$, 300 MHz): 3.36 (d, J = 14.24 Hz, 1H), 3.87 (s, 3H), 3.91 (s, 2H), 4.01 (dd, J_1 = 4.34 Hz, J_2 = 14.18 Hz, 1H), 5.87 (d, J = 9.88 Hz, 1H), 6.98 (d, J = 6.34 Hz, 2H), 7.22 (d, J = 4.54 Hz, 2H), 7.54 (d, J = 6.34 Hz, 2H), 7.96 (d, J = 8.46 Hz, 2H). ESI-MS: 386.87 ($C_{19}H_{17}ClN_3O_2S$, $[M+H]^+$). Anal. Calcd for $C_{19}H_{16}ClN_3O_2S$: C, 59.14; H, 4.18; N, 10.89. Found: C, 59.28; H, 4.20; N, 10.97.

4.2.3.19. 2-(3-(4-Bromophenyl)-5-phenyl-4,5-dihydro-1*H* -pyrazol-1-yl)thiazol-4(5*H*)-one (E20). Yield 72%; mp 242–244 °C. ^{1}H NMR ($CDCl_3$, 300 MHz): 3.37 (d, J = 14.08 Hz, 1H), 3.87 (s, 2H), 3.98 (dd, J_1 = 4.48 Hz, J_2 = 10.34 Hz, 1H), 5.85 (d, J = 8.56 Hz, 1H), 7.25–7.35 (m, 3H), 7.42 (d, J = 5.85 Hz, 2H), 7.60 (d, J = 6.34 Hz, 2H), 7.72 (d, J = 14.18 Hz, 2H). ESI-MS: 401.29 ($C_{18}H_{15}BrN_3OS$, $[M+H]^+$). Anal. Calcd for $C_{18}H_{14}BrN_3OS$: C, 54.01; H, 3.53; N, 10.50. Found: C, 54.18; H, 3.55; N, 10.57.

4.2.3.20. 2-(3-(4-Bromophenyl)-5-(4-fluorophenyl)-4,5-dihydro-1*H* -pyrazol-1-yl)thiazol-4(5*H*)-one (E20). Yield 84%; mp 250–252 °C. ^{1}H NMR ($CDCl_3$, 300 MHz): 3.33 (d, J = 15.18 Hz, 1H), 3.87–3.93 (m, 3H), 5.83 (d, J = 8.58 Hz, 1H), 6.99–7.05 (m, 2H), 7.21–7.25 (m, 2H), 7.64 (dd, J_1 = 8.61 Hz, J_2 = 17.58 Hz, 4H). ESI-MS: 419.28 ($C_{18}H_{14}BrFN_3OS$, $[M+H]^+$). Anal. Calcd for $C_{18}H_{13}BrFN_3OS$: C, 51.69; H, 3.13; N, 10.05. Found: C, 51.86; H, 3.14; N, 10.13.

4.2.3.21. 2-(3-(4-Bromophenyl)-5-(4-chlorophenyl)-4,5-dihydro-1*H* -pyrazol-1-yl)thiazol-4(5*H*)-one (E21). Yield 86%; mp 256–258 °C. ^{1}H NMR ($CDCl_3$, 300 MHz): 3.32 (d, J = 17.37 Hz, 1H), 3.71 (s, 2H), 3.87 (dd, J_1 = 6.78 Hz, J_2 = 13.56 Hz, 1H), 5.83 (s, 1H), 7.19 (d, J = 8.43 Hz, 2H), 7.31(d, J = 8.07 Hz, 2H), 7.59–7.66 (m, 4H). ESI-MS: 435.74 ($C_{18}H_{14}BrClN_3OS$, $[M+H]^+$). Anal. Calcd for $C_{18}H_{13}BrClN_3OS$: C, 49.73; H, 3.01; N, 9.67. Found: C, 49.86; H, 3.02; N, 9.72.

4.2.3.22. 2-(3,5-Bis(4-bromophenyl)-4,5-dihydro-1*H*-pyrazol-1-yl)thiazol-4(5*H*)-one (E22). Yield 85%; mp 266–268 °C. ^{1}H NMR ($CDCl_3$, 300 MHz): 3.31 (d, J = 17.91 Hz, 1H), 3.87 (s, 2H), 3.95 (dd, J_1 = 6.42 Hz, J_2 = 17.37 Hz, 1H), 5.75 (d, J = 8.04 Hz, 1H), 7.12 (d, J = 8.25 Hz, 2H), 7.46 (d, J = 8.22 Hz, 2H), 7.59–7.67 (m, 4H). ESI-MS: 480.19 ($C_{18}H_{14}Br_2N_3OS$, $[M+H]^+$). Anal.Calcd for $C_{18}H_{13}Br_2N_3OS$: C, 45.12; H, 2.73; N, 8.77. Found: C, 45.21; H, 2.72; N, 8.83.

4.2.3.23. 2-(3-(4-Bromophenyl)-5-(4-chlorophenyl)-4,5-dihydro-1*H* -pyrazol-1-yl)thiazol-4(5*H*)-one (E23). Yield 84%; mp 238–240 °C. ^{1}H NMR ($CDCl_3$, 300 MHz): 2.31 (s, 3H), 3.34 (dd, J_1 = 3.84 Hz, J_2 = 17.91 Hz, 1H), 3.85 (s, 2H), 3.91 (dd, J_1 = 5.94 Hz, J_2 = 10.78 Hz, 1H), 5.82 (dd, J_1 = 3.84, J_2 = 11.16 Hz, 1H), 7.13–7.19 (m, 4H), 7.59–7.68 (m, 4H). ESI-MS: 415.32 ($C_{19}H_{17}BrN_3OS$, $[M+H]^+$). Anal. Calcd for $C_{19}H_{16}BrN_3OS$: C, 55.08; H, 3.89; N, 10.14. Found: C, 55.16; H, 3.88; N, 10.19.

4.2.3.24. 2-(3-(4-Bromophenyl)-5-(4-methoxyphenyl)-4,5-dihydro-1*H* -pyrazol-1-yl)thiazol-4(5*H*)-one (E24). Yield 86%; mp 240–242 °C. ^{1}H NMR ($CDCl_3$, 300 MHz): 3.35 (dd, J_1 = 4.24 Hz, J_2 = 17.82 Hz, 1H), 3.78 (s, 3H), 3.85–3.97 (m, 3H), 5.82 (d, J = 7.32 Hz, 1H), 6.85 (d, J = 8.61 Hz, 2H), 7.20 (d, J = 8.61 Hz, 2H), 7.55–7.62 (m, 4H). ESI-MS: 431.32 ($C_{19}H_{17}BrN_3O_2S$, $[M+H]^+$). Anal. Calcd for $C_{19}H_{16}BrN_3O_2S$: C, 53.03; H, 3.75; N, 9.76. Found: C, 53.17; H, 3.77; N, 9.83.

4.2.3.25. 2-(5-Phenyl-3-*p*-tolyl-4,5-dihydro-1*H*-pyrazol-1-yl)thiazol-4(5*H*)-one (E25). Yield 63%; mp 210–212 °C. ^{1}H NMR ($CDCl_3$, 300 MHz): 2.43 (s, 3H), 3.36 (dd, J_1 = 4.08 Hz, J_2 = 16.84 Hz, 1H), 3.87 (s, 2H), 3.97 (dd, J_1 = 5.35 Hz, J_2 = 14.24 Hz, 1H), 5.89 (d, J = 6.48 Hz, 1H), 7.25–7.35 (m, 3H), 7.27–7.30 (m, 4H), 7.45 (d, J = 5.34 Hz, 2H), 7.72 (d, J = 6.94 Hz, 2H). ESI-MS: 336.42 ($C_{19}H_{18}N_3OS$, $[M+H]^+$). Anal. Calcd for $C_{19}H_{17}N_3OS$: C, 68.03; H, 5.11; N, 12.53. Found: C, 68.16; H, 5.14; N, 12.63.

4.2.3.26. 2-(5-(4-Fluorophenyl)-3-(*p*-tolyl)-4,5-dihydro-1*H*-pyrazol-1-yl)thiazol-4 (5*H*)-one (E26). Yield 78%; mp 228–230 °C. ^{1}H NMR ($CDCl_3$, 300 MHz): 2.43 (s, 3H), 3.34 (dd, J_1 = 3.63 Hz, J_2 = 17.53 Hz, 1H), 3.87(s, 2H), 3.94 (dd, J_1 = 6.25 Hz, J_2 = 12.84 Hz, 1H), 5.85(d, J = 7.32 Hz, 1H), 6.98–7.04 (m, 2H), 7.23 (s, 2H), 7.28 (d, J = 4.16 Hz, 2H), 7.69 (d, J = 8.22 Hz, 2H). ESI-MS: 354.41 ($C_{19}H_{17}FN_3OS$, $[M+H]^+$). Anal.Calcd for $C_{19}H_{16}FN_3OS$: C, 64.57; H, 4.56; N, 11.89. Found: C, 64.68; H, 4.58; N, 11.95.

4.2.3.27. 2-(5-(4-Chlorophenyl)-3-(*p*-tolyl)-4,5-dihydro-1*H*-pyrazol-1-yl)thiazol-4 (5*H*)-one (E27). Yield 81%; mp 234–236 °C. ^{1}H NMR ($CDCl_3$, 300 MHz): 2.40 (s, 3H), 3.15 (dd, J_1 = 3.84 Hz, J_2 = 17.73 Hz, 1H), 3.76 (s, 2H), 3.83 (dd, J_1 = 11.52, J_2 = 17.73 Hz, 1H), 5.99 (dd, J_1 = 3.66 Hz, J_2 = 11.52 Hz, 1H), 7.16 (d, J = 8.4 Hz, 2H), 7.23–7.26 (m, 2H), 7.28–7.31 (m, 2H), 7.61 (d, J = 6.42 Hz, 2H). ESI-MS: 370.87 ($C_{19}H_{17}ClN_3OS$, $[M+H]^+$). Anal. Calcd for $C_{19}H_{16}ClN_3OS$: C, 61.70; H, 4.36; N, 11.36. Found: C, 61.82; H, 4.34; N, 11.43.

4.2.3.28. 2-(5-(4-Bromophenyl)-3-*p*-tolyl-4,5-dihydro-1*H* -pyrazol-1-yl)thiazol-4(5*H*)-one (E28). Yield 83%; mp 245–247 °C. ^{1}H NMR ($CDCl_3$, 300 MHz): 2.42 (s, 3H), 3.33 (d, J = 8.79 Hz, 1H), 3.90 (s, 2H), 3.95 (dd, J_1 = 6.60 Hz, J_2 = 10.62 Hz, 1H), 5.86 (d, J = 4.68 Hz, 1H), 7.16 (d, J = 5.04 Hz, 2H), 7.26–7.28 (m, 2H), 7.46(d, J = 5.04 Hz, 2H), 7.69 (d, J = 4.86 Hz, 1H). ESI-MS: 415.32 ($C_{19}H_{17}BrN_3OS$, $[M+H]^+$). Anal. Calcd for $C_{19}H_{16}BrN_3OS$: C, 55.08; H, 3.89; N, 10.14. Found: C, 55.21; H, 3.92; N, 10.20.

4.2.3.29. 2-(3,5-Dip-tolyl-4,5-dihydro-1*H*-pyrazol-1-yl)thiazol-4(5*H*)-one (E29). Yield 75%; mp 220–222 °C. ^{1}H NMR ($CDCl_3$, 300 MHz): 2.43 (s, 6H), 3.36 (dd, J_1 = 4.08 Hz, J_2 = 16.98 Hz, 1H), 3.86 (s, 2H), 4.08 (dd, J_1 = 6.94 Hz, J_2 = 15.08 Hz, 1H), 5.86 (d, J = 10.08 Hz, 1H), 7.16–7.20 (m, 4H), 7.27 (d, J = 5.88 Hz, 2H), 7.72 (d, J = 9.02 Hz, 2H). ESI-MS: 350.45 ($C_{20}H_{20}N_3OS$, $[M+H]^+$). Anal. Calcd for $C_{20}H_{19}N_3OS$: C, 68.74; H, 5.48; N, 12.02. Found: C, 68.86; H, 5.51; N, 12.11.

4.2.3.30. 2-(5-(4-Methoxyphenyl)-3-(p-tolyl)-4,5-dihydro-1*H* -pyrazol-1-yl)thiazol-4(5*H*)-one (E30). Yield 84%; mp 224–226 °C. ^{1}H NMR ($CDCl_3$, 300 MHz): 2.42 (s, 3H), 3.36 (dd, J_1 = 3.66 Hz, J_2 = 17.94 Hz, 1H), 3.77 (s, 3H), 3.86 (s, 2H), 4.12 (dd, J_1 = 7.28 Hz, J_2 = 14.14 Hz, 1H), 5.79 (s, 1H), 6.84 (d, J = 8.58 Hz, 2H), 7.20 (d, J = 8.62 Hz, 2H), 7.27 (d, J = 6.96 Hz, 2H), 7.70 (d, J = 8.25 Hz, 2H). ESI-MS: 366.45 ($C_{20}H_{20}N_3O_2S$, $[M+H]^+$). Anal. Calcd for $C_{20}H_{19}N_3O_2S$: C, 65.73; H, 5.24; N, 11.50. Found: C, 65.55; H, 5.21; N, 11.41.

4.2.3.31. 2-(3-(4-Methoxyphenyl)-5-phenyl-4,5-dihydro-1*H*-pyrazol-1-yl)thiazol-4(5*H*)-one (E31). Yield 68%; mp 205–207 °C. ^{1}H NMR ($CDCl_3$, 300 MHz): 3.72 (d, J = 14.02 Hz, 1H), 3.85–3.97 (m, 5H), 4.02 (dd, J_1 = 8.02 Hz, J_2 = 15.48 Hz, 1H), 5.86 (s, 1H), 7.11 (d, J = 6.18 Hz, 2H), 7.25–7.30 (m, 3H), 7.42 (d, J = 5.44 Hz, 2H), 7.93 (d, J = 8.24 Hz, 2H). ESI-MS: 352.42 ($C_{19}H_{18}N_3O_2S$, $[M+H]^+$). Anal. Calcd for $C_{19}H_{17}N_3O_2S$: C, 64.94; H, 4.88; N, 11.96. Found: C, 65.12; H, 4.89; N, 12.03.

4.2.3.32. 2-(5-(4-Fluorophenyl)-3-(4-methoxyphenyl)-4,5-dihydro-1*H* -pyrazol-1-yl)thiazol-4(5*H*)-one (E32). Yield 83%; mp 210–212 °C. ^{1}H NMR ($CDCl_3$, 300 MHz): 3.77 (s, 1H), 3.85–3.97 (m, 6H), 5.84 (s, 1H), 6.84 (d, J = 8.04 Hz, 1H), 6.96–7.04 (m, 4H), 7.21–7.32 (m, 1H), 7.75 (d, J = 8.76 Hz, 2H). ESI-MS: 370.41 ($C_{19}H_{17}FN_3O_2S$, $[M+H]^+$). Anal. Calcd for $C_{19}H_{16}FN_3O_2S$: C, 61.77; H, 4.37; N, 11.37. Found: C, 61.86; H,4.36; N, 11.43.

4.2.3.33. 2-(5-(4-Chlorophenyl)-3-(4-methoxyphenyl)-4,5-dihydro-1*H* -pyrazol-1-yl)thiazol-4(5*H*)-one (E33). Yield 84%; mp 224–226 °C. ^{1}H NMR ($CDCl_3$, 300 MHz): 3.71 (dd, J_1 = 6.96 Hz, J_2 = 13.89 Hz, 1H), 3.85–3.90 (m, 5H), 4.11(dd, J_1 = 7.14 Hz, J_2 = 14.25 Hz, 1H), 5.79 (s, 1H), 6.97 (d, J = 8.61 Hz, 2H), 7.21 (d, J = 8.22 Hz, 2H), 7.30 (d, J = 8.22 Hz, 2H), 7.74 (d, J = 8.79 Hz, 2H). ESI-MS: 386.87 ($C_{19}H_{17}ClN_3O_2S$, $[M+H]^+$). Anal. Calcd for $C_{19}H_{16}ClN_3O_2S$: C, 59.14; H, 4.18; N, 10.89. Found: C,59.29; H,4.20; N, 10.96.

4.2.3.34. 2-(5-(4-Bromophenyl)-3-(4-methoxyphenyl)-4,5-dihydro-1*H* -pyrazol-1-yl)thiazol-4(5*H*)-one (E34). Yield 88%; mp 230–232 °C. ^{1}H NMR ($CDCl_3$, 300 MHz): 3.36(d, J = 10.04 Hz, 1H), 3.85–3.96 (m, 5H), 4.08 (dd, J_1 = 7.14 Hz, J_2 = 14.25 Hz, 1H), 5.79 (s, 1H), 6.91–6.98 (m, 2H), 7.15 (s, 2H), 7.46 (s, 2H), 7.74 (d, J = 6.39 Hz, 2H). ESI-MS: 431.32 ($C_{19}H_{17}BrN_3O_2S$, $[M+H]^+$). Anal. Calcd for $C_{19}H_{16}BrN_3O_2S$: C, 53.03; H, 3.75; N, 9.76. Found: C, 53.16; H, 3.77; N, 9.82.

4.2.3.35. 2-(3-(4-Methoxyphenyl)-5-(p-tolyl)-4,5-dihydro-1*H* -pyrazol-1-yl)thiazol-4(5*H*)-one (E35). Yield 80%; mp 217–219 °C. ^{1}H NMR ($CDCl_3$, 300 MHz): 2.31 (s, 3H), 3.35 (d, J = 16.83 Hz, 1H), 3.84–3.95 (m, 6H), 5.82 (d, J = 8.61 Hz, 1H), 6.97 (d, J = 8. 10 Hz, 2H), 7.11–7.18 (m, 4H), 7.74 (d, J = 8.43 Hz, 2H). ESI-MS: 366.45 ($C_{20}H_{20}N_3O_2S$, $[M+H]^+$). Anal. Calcd for $C_{20}H_{19}N_3O_2S$: C, 65.73; H, 5.24; N, 11.50. Found: C, 65.56; H, 5.22; N, 11.42.

4.2.3.36. 2-(3-(4-Chlorophenyl)-5-phenyl-4,5-dihydro-1*H* -pyrazol-1-yl)thiazol-4(5*H*)-one (E36). Yield 85%; mp 220–222 °C. ^{1}H NMR ($CDCl_3$, 300 MHz): 3.36 (dd, J_1 = 3.48 Hz, J_2 = 17.73 Hz, 1H), 3.92 (s, 2H), 4.13 (dd, J_1 = 4.38 Hz, J_2 = 15.78 Hz, 1H), 5.88 (d,

J = 10.95 Hz, 1H), 6.84 (d, J = 8.79 Hz, 2H), 6.97 (d, J = 8.79 Hz, 2H), 7.21–7.26 (m, 2H), 7.76 (d, J = 8.97 Hz, 2H). ESI-MS: 382.45 ($C_{20}H_{20}N_3O_3S$, $[M+H]^+$). Anal. Calcd for $C_{20}H_{19}N_3O_3S$: C, 62.97; H, 5.02; N, 11.02. Found: C, 63.05; H, 5.05; N, 11.07.

4.3. Preparation, purification of HER-2 and EGFR and inhibitory assay

A 1.7 kb cDNA encoded for human HER-2 cytoplasmic domain (HER-2-CD, amino acids 676–1245) and 1.6 kb cDNA encoded for the EGFR cytoplasmic domain (EGFR-CD, amino acids 645–1186) were cloned into baculoviral expression vectors pBlueBacHis2B and pFASTBacHTc (Huakang Company, China), separately. A sequence that encodes $(His)_6$ was located at the 50 upstream to the HER-2 and EGFR sequences. Sf-9 cells were infected for 3 days for protein expression. Sf-9 cell pellets were solubilized at 0 °C in a buffer at pH 7.4 containing 50 mM HEPES, 10 mM NaCl, 1% Triton, 10 μM ammonium molybdate, 100 μM sodium vanadate, 10 μg/mL aprotinin, 10 μg/mL leupeptin, 10 μg/mL pepstatin, and 16 μg/mL benzamidine HCl for 20 min followed by 20 min centrifugation. Crude extract supernatant was passed through an equilibrated Ni-NTA superflow packed column and washed with 10 mM and then 100 mM imidazole to remove nonspecifically bound material. Histidine tagged proteins were eluted with 250 and 500 mM imidazole and dialyzed against 50 mM NaCl, 20 mM HEPES, 10% glycerol, and 1 μg/mL each of aprotinin, leupeptin, and pepstatin for 2 h. The entire purification procedure was performed at 4 °C or on ice.

Both EGFR and HER-2 kinase assays were set up to assess the level of autophosphorylation based on DELFIA/Time-Resolved Fluorometry. Compounds **E1–E36** were dissolved in 100% DMSO and diluted to the appropriate concentrations with 25 mM HEPES at pH 7.4. In each well, 10 μL compound was incubated with 10 μL (12.5 ng for HER-2 or 5 ng for EGFR) recombinant enzyme (1:80 dilution in 100 mM HEPES) for 10 min at room temperature. Then, 10 μL of 5 mM buffer (containing 20 mM HEPES, 2 mM $MnCl_2$, 100 μM Na_3VO_4, and 1 mM DTT) and 20 μL of 0.1 mM ATP–50 mM $MgCl_2$ were added for 1 h. Positive and negative controls were included in each plate by incubation of enzyme with or without ATP-$MgCl_2$. At the end of incubation, liquid was aspirated, and plates were washed three times with wash buffer. A 75 μL (400 ng) sample of europium labeled anti-phosphotyrosine antibody was added to each well for another 1 h of incubation. After washing, enhancement solution was added and the signal was detected by Victor (Wallac Inc.) with excitation at 340 nm and emission at 615 nm. The percentage of autophosphorylation inhibition by the compounds was calculated using the following formula: 100%−[(negative control)/(positive control−negative control)]. The IC_{50} was obtained from curves of percentage inhibition with eight concentrations of compound. As the contaminants in the enzyme preparation are fairly low, the majority of the signal detected by the anti-phosphotyrosine antibody is from EGFR or HER-2.

4.4. Antiproliferation assay

The antiproliferative activities of the prepared compounds against MCF-7, B16-F10 and HCT-116 cells were evaluated as described elsewhere with some modifications.[31] Target tumor cell lines were grown to log phase in RPMI 1640 medium supplemented with 10% fetal bovine serum. After diluting to 2×10^4 cells mL^{-1} with the complete medium, 100 μL of the obtained cell suspension was added to each well of 96-well culture plates. The subsequent incubation was permitted at 37 °C, 5% CO_2 atmosphere for 24 h before the cytotoxicity assessments. Tested samples at pre-set concentrations were added to six wells with erlotinib as positive reference. After 48 h exposure period, 40 μL of PBS containing 2.5 mg mL^{-1} of MTT (3-(4,5-dimethylthiazol-2-yl)-2,5-diphenyltetrazolium bromide)) was added to each well. Four hours later, 100 μL extraction solution (10% SDS–5% isobutyl alcohol–0.01 M HCl) was added. After an overnight incubation at 37 °C, the optical density was measured at a wavelength of 570 nm on an ELISA microplate reader. In all experiments three replicate wells were used for each drug concentration. Each assay was carried out for at least three times. The results were summarized in Table 3.

4.5. Molecular docking study

Molecular docking of compounds into the 3D EGFR complex structure (PDB code: 1M17) was carried out using the Discovery Stutio (version 3.1) as implemented through the graphical user interface DS-LigandFit protocal.

The three-dimensional structures of the aforementioned compounds were constructed using Chem 3D ultra 11.0 software [Chemical Structure Drawing Standard; Cambridge Soft corporation, USA (2009)], then they were energetically minimized by using MOPAC with 100 iterations and minimum RMS gradient of 0.10. The crystal structures of EGFR complex were retrieved from the RCSB Protein Data Bank (http://www.rcsb.org/pdb/home/home.do). All bound water and ligands were eliminated from the protein and the polar hydrogen was added. The whole EGFR complex was defined as a receptor and the site sphere was selected based on the ligand binding location of ATP, then the ATP molecule was removed and **E28** was placed during the molecular docking procedure. Types of interactions of the docked protein with ligand were analyzed after the end of molecular docking.

Acknowledgment

This work was supported by The National Natural Science Foundation of China (NSFC J1103512).

References and notes

1. Zhang, X. W.; Gureasko, J.; Shen, K.; Cole, P. A.; Kuriyan *J. Cell* **2006**, *125*, 1137.
2. Kolibaba, K. S.; Druker, B. *J. Biochim. Biophys. Acta* **1997**, *21*, 1333.
3. Fleming, T. P.; Saxena, A.; Clark, W. C.; Robertson, J. T.; Oldfield, E. H.; Aaronson, S. A.; Ali, I. U. *Cancer Res.* **1992**, *52*, 4550.
4. Jensen, P. B.; Hunter, T. *Nature* **2001**, *411*, 355.
5. Kim, H.; Muller, W. *J. Exp. Cell Res.* **1999**, *253*, 78.
6. Moscatello, D. K.; Holgado-Mudruga, M.; Godwin, A. K.; Ramirez, G.; Gunn, G.; Zoltick, P. W.; Biegel, J. A.; Hayes, R. L.; Wong, A. J. *Cancer Res.* **1995**, *55*, 5536.
7. Luo, Y.; Li, Y.; Qiu, K. M.; Lu, X.; Fu, J.; Zhu, H. L. *Bioorg. Med. Chem.* **2011**, *19*, 6069.
8. Ciardiello, F.; Tortola, G. *Clin. Cancer Res.* **2001**, *7*, 2958.
9. Bridges, A. J. *Curr. Med. Chem.* **1999**, *6*, 825.
10. Boschelli, D. H. *Drugs Future* **1999**, *24*, 515.
11. Anido, J.; Matar, P.; Albanell, J.; Guzman, M.; Rojo, F.; Arribas, J.; Averbuch, S.; Baselga, J. *Clin. Cancer Res.* **2003**, *9*, 1274.
12. Chandregowda, V.; Rao, G. V.; Reddy, G. C. *Org. Process Res. Dev.* **2007**, *11*, 813.
13. Manfredini, S.; Bazzanini, R.; Baraldi, P. G.; Guarneri, M.; Simoni, D.; Marongiu, M. E.; Pani, A.; Tramontano, E.; La Colla, P. *J. Med. Chem.* **1992**, *35*, 917.
14. Manfredini, S.; Bazzanini, R.; Baraldi, P. G.; Bonora, M.; Marangoni, M.; Simoni, D.; Pani, A.; Scintu, F.; Pinna, E. *Anti-Cancer Drug Des.* **1996**, *11*, 193.
15. Park, H.-A.; Lee, K.; Park, S.-J.; Ahn, B.; Lee, J.-C.; Cho, H. Y.; Lee, K.-I. *Bioorg. Med. Chem. Lett.* **2005**, *15*, 3307.
16. Tanitame, A.; Oyamada, Y.; Ofuji, K.; Fujimoto, M.; Iwai, N.; Hiyama, Y.; Suzuki, K.; Ito, H.; Wachi, M.; Yamagishi, J. *J. Med. Chem.* **2004**, *47*, 3693.
17. Kucukguzel, S. G.; Rollas, S.; Erdeniz, H.; Kiraz, M.; Ekinci, A. C.; Vidin, A. *Eur. J. Med. Chem.* **2000**, *35*, 761.
18. Penning, T. D.; Talley, J. J.; Bertenshaw, S. R.; Carter, J. S.; Collins, P. W.; Docter, S.; Graneto, M. J.; Lee, L. F.; Malecha, J. W.; Miyashiro, J. M.; Rogers, R. S.; Rogier, D. J.; Yu, S. S.; Anderson, G. D.; Burton, E. G.; Cogburn, J. N.; Gregory, S. A.; Koboldt, C. M.; Perkins, W. E.; Seibert, K.; Veenhuizen, A. W.; Zhang, Y. Y.; Isakson, P. C. *J. Med. Chem.* **1997**, *40*, 1347.
19. Menozzi, G.; Mosti, L.; Fossa, P.; Mattioli, F.; Ghia, M. *J. Heterocycl. Chem.* **1997**, *34*, 963.
20. Sridhar, R.; Perumal, P. T.; Etti, S.; Shanmugam, G.; Ponnuswamy, M. N.; Prabavathy, V. R.; Mathivanan, N. *Bioorg. Med. Chem. Lett.* **2004**, *14*, 6035.

21. Bebernitz, G. R.; Argentieri, G.; Battle, B.; Brennan, C.; Balkan, B.; Burkey, B. F.; Eckhardt, M.; Gao, J.; Kapa, P.; Strohschein, R. J.; Schuster, H. F.; Wilson, M.; Xu, D. D. *J. Med. Chem.* **2001**, *44*, 2601.
22. Ducray, R.; Ballard, P.; Barlaam, B. C.; Hickinson, M. D.; Kettle, J. G.; Ogilvie, D. J.; Trigwell, C. B. *Bioorg. Med. Chem. Lett.* **2008**, *18*, 959.
23. Lv, P. C.; Li, H. Q.; Suan, J.; Zhou, Y.; Zhu, H. L. *Bioorg. Med. Chem.* **2010**, *18*, 4606.
24. Ottana, R.; Maccari, R.; Barreca, M. L.; Bruno, G.; Rotondo, A.; Rossi, A.; Chiricosta, G.; Di Paola, R.; Sautebin, L.; Cuzzocrea, S.; Vigorita, M. G. *Bioorg. Med. Chem.* **2005**, *13*, 4243.
25. Gududuru, V.; Hurh, E.; Dalton, J. T.; Miller, D. D. *Bioorg. Med. Chem. Lett.* **2004**, *14*, 5289.
26. Rydzik, E.; Szadowska, A.; Kaminska, A. *Acta Pol. Pharm.* **1984**, *41*, 459.
27. Havrylyuk, D.; Mosula, L.; Zimenkovsky, B.; Vasylenko, O.; Gzella, A.; Lesyk, R. *Eur. J. Med. Chem.* **2010**, *45*(5012), e5021.
28. Lv, P. C.; Zhou, C. F.; Chen, J.; Liu, P. G.; Wang, K. R.; Mao, W. J.; Li, H. Q.; Yang, Y.; Xiong Zhu, J.; Zhu, H. L. *Bioorg. Med. Chem* **2010**, *18*, 314.
29. Dayam, R.; Aiello, F.; Deng, J. X.; Wu, Y.; Garofalo, A.; Chen, X. Y.; Neamati, N. *J. Med. Chem.* **2006**, *49*, 4526.
30. Manfredini, S.; Bazzanini, R.; Baraldi, P. G.; Bonora, M.; Marangoni, M.; Simoni, D.; Pani, A.; Scintu, F.; Pinna, E. *Anti-Cancer Drug Des.* **1996**, *11*, 193.
31. Boumendjel, A.; Boccard, J.; Carrupt, P.-A.; Nicolle, E.; Blanc, M.; Geze, A.; Choisnard, L.; Wouessidjewe, D.; Matera, E. L.; Dumontet, C. *J. Med. Chem.* **2008**, *51*, 2307.